arXiv:1402.7134v1 [hep-ex] 28 Feb 2014

# Measurement of the Lepton Forward-Backward Asymmetry in Inclusive $B \to X_s \ell^+ \ell^-$ Decays

Y. Sato,[61] A. Ishikawa,[61] H. Yamamoto,[61] A. Abdesselam,[56] I. Adachi,[12] K. Adamczyk,[42] H. Aihara,[62] D. M. Asner,[47] V. Aulchenko,[4] T. Aushev,[20] R. Ayad,[56] A. M. Bakich,[55] A. Bala,[48] V. Bhardwaj,[38] B. Bhuyan,[14] A. Bondar,[4] G. Bonvicini,[68] A. Bozek,[42] M. Bračko,[31,21] T. E. Browder,[11] D. Červenkov,[5] V. Chekelian,[32] A. Chen,[39] B. G. Cheon,[10] I.-S. Cho,[70] K. Cho,[25] V. Chobanova,[32] Y. Choi,[54] D. Cinabro,[68] J. Dalseno,[32,58] M. Danilov,[20,34] Z. Doležal,[5] Z. Drásal,[5] A. Drutskoy,[20,34] D. Dutta,[14] K. Dutta,[14] S. Eidelman,[4] H. Farhat,[68] J. E. Fast,[47] T. Ferber,[8] V. Gaur,[57] A. Garmash,[4] R. Gillard,[68] Y. M. Goh,[10] B. Golob,[29,21] J. Haba,[12] T. Hara,[12] K. Hayasaka,[37] H. Hayashii,[38] X. H. He,[49] Y. Hoshi,[60] W.-S. Hou,[41] H. J. Hyun,[27] T. Iijima,[37,36] R. Itoh,[12] Y. Iwasaki,[12] T. Iwashita,[24] I. Jaegle,[11] T. Julius,[33] J. H. Kang,[70] E. Kato,[61] Y. Kato,[36] H. Kawai,[6] T. Kawasaki,[44] H. Kichimi,[12] D. Y. Kim,[53] H. J. Kim,[27] J. B. Kim,[26] J. H. Kim,[25] M. J. Kim,[27] Y. J. Kim,[25] K. Kinoshita,[7] J. Klucar,[21] B. R. Ko,[26] P. Kodyš,[5] S. Korpar,[31,21] P. Križan,[29,21] P. Krokovny,[4] T. Kuhr,[23] T. Kumita,[64] A. Kuzmin,[4] Y.-J. Kwon,[70] S.-H. Lee,[26] Y. Li,[67] J. Libby,[15] C. Liu,[52] Y. Liu,[7] Z. Q. Liu,[16] D. Liventsev,[12] P. Lukin,[4] H. Miyata,[44] R. Mizuk,[20,34] G. B. Mohanty,[57] A. Moll,[32,58] R. Mussa,[19] M. Nakao,[12] Z. Natkaniec,[42] M. Nayak,[15] E. Nedelkovska,[32] N. K. Nisar,[57] S. Nishida,[12] O. Nitoh,[65] S. Ogawa,[59] P. Pakhlov,[20,34] H. Park,[27] H. K. Park,[27] T. K. Pedlar,[30] T. Peng,[52] R. Pestotnik,[21] M. Petrič,[21] L. E. Piilonen,[67] E. Ribežl,[21] M. Ritter,[32] M. Röhrken,[23] A. Rostomyan,[8] H. Sahoo,[11] T. Saito,[61] Y. Sakai,[12] S. Sandilya,[57] D. Santel,[7] L. Santelj,[21] T. Sanuki,[61] V. Savinov,[50] O. Schneider,[28] G. Schnell,[1,13] C. Schwanda,[17] A. J. Schwartz,[7] R. Seidl,[51] D. Semmler,[9] K. Senyo,[69] M. E. Sevior,[33] M. Shapkin,[18] C. P. Shen,[2] T.-A. Shibata,[63] J.-G. Shiu,[41] B. Shwartz,[4] A. Sibidanov,[55] F. Simon,[32,58] Y.-S. Sohn,[70] A. Sokolov,[18] E. Solovieva,[20] S. Stanič,[45] M. Starič,[21] T. Sumiyoshi,[64] U. Tamponi,[19,66] G. Tatishvili,[47] Y. Teramoto,[46] K. Trabelsi,[12] M. Uchida,[63] S. Uehara,[12] T. Uglov,[20,35] Y. Unno,[10] S. Uno,[12] P. Urquijo,[3] Y. Ushiroda,[12] Y. Usov,[4] S. E. Vahsen,[11] C. Van Hulse,[1] P. Vanhoefer,[32] G. Varner,[11] K. E. Varvell,[55] V. Vorobyev,[4] C. H. Wang,[40] M.-Z. Wang,[41] P. Wang,[16] X. L. Wang,[67] Y. Watanabe,[22] E. Won,[26] J. Yamaoka,[47] Y. Yamashita,[43] S. Yashchenko,[8] Y. Yook,[70] Z. P. Zhang,[52] V. Zhilich,[4] V. Zhulanov,[4] and A. Zupanc[21]

(The Belle Collaboration)

[1] *University of the Basque Country UPV/EHU, 48080 Bilbao*
[2] *Beihang University, Beijing 100191*
[3] *University of Bonn, 53115 Bonn*
[4] *Budker Institute of Nuclear Physics SB RAS and Novosibirsk State University, Novosibirsk 630090*
[5] *Faculty of Mathematics and Physics, Charles University, 121 16 Prague*
[6] *Chiba University, Chiba 263-8522*
[7] *University of Cincinnati, Cincinnati, Ohio 45221*
[8] *Deutsches Elektronen–Synchrotron, 22607 Hamburg*
[9] *Justus-Liebig-Universität Gießen, 35392 Gießen*
[10] *Hanyang University, Seoul 133-791*
[11] *University of Hawaii, Honolulu, Hawaii 96822*
[12] *High Energy Accelerator Research Organization (KEK), Tsukuba 305-0801*
[13] *IKERBASQUE, Basque Foundation for Science, 48011 Bilbao*
[14] *Indian Institute of Technology Guwahati, Assam 781039*
[15] *Indian Institute of Technology Madras, Chennai 600036*
[16] *Institute of High Energy Physics, Chinese Academy of Sciences, Beijing 100049*
[17] *Institute of High Energy Physics, Vienna 1050*
[18] *Institute for High Energy Physics, Protvino 142281*
[19] *INFN - Sezione di Torino, 10125 Torino*
[20] *Institute for Theoretical and Experimental Physics, Moscow 117218*
[21] *J. Stefan Institute, 1000 Ljubljana*
[22] *Kanagawa University, Yokohama 221-8686*
[23] *Institut für Experimentelle Kernphysik, Karlsruher Institut für Technologie, 76131 Karlsruhe*
[24] *Kavli Institute for the Physics and Mathematics of the Universe (WPI), University of Tokyo, Kashiwa 277-8583*
[25] *Korea Institute of Science and Technology Information, Daejeon 305-806*
[26] *Korea University, Seoul 136-713*
[27] *Kyungpook National University, Daegu 702-701*
[28] *École Polytechnique Fédérale de Lausanne (EPFL), Lausanne 1015*
[29] *Faculty of Mathematics and Physics, University of Ljubljana, 1000 Ljubljana*
[30] *Luther College, Decorah, Iowa 52101*
[31] *University of Maribor, 2000 Maribor*

[32] Max-Planck-Institut für Physik, 80805 München
[33] School of Physics, University of Melbourne, Victoria 3010
[34] Moscow Physical Engineering Institute, Moscow 115409
[35] Moscow Institute of Physics and Technology, Moscow Region 141700
[36] Graduate School of Science, Nagoya University, Nagoya 464-8602
[37] Kobayashi-Maskawa Institute, Nagoya University, Nagoya 464-8602
[38] Nara Women's University, Nara 630-8506
[39] National Central University, Chung-li 32054
[40] National United University, Miao Li 36003
[41] Department of Physics, National Taiwan University, Taipei 10617
[42] H. Niewodniczanski Institute of Nuclear Physics, Krakow 31-342
[43] Nippon Dental University, Niigata 951-8580
[44] Niigata University, Niigata 950-2181
[45] University of Nova Gorica, 5000 Nova Gorica
[46] Osaka City University, Osaka 558-8585
[47] Pacific Northwest National Laboratory, Richland, Washington 99352
[48] Panjab University, Chandigarh 160014
[49] Peking University, Beijing 100871
[50] University of Pittsburgh, Pittsburgh, Pennsylvania 15260
[51] RIKEN BNL Research Center, Upton, New York 11973
[52] University of Science and Technology of China, Hefei 230026
[53] Soongsil University, Seoul 156-743
[54] Sungkyunkwan University, Suwon 440-746
[55] School of Physics, University of Sydney, NSW 2006
[56] Department of Physics, Faculty of Science, University of Tabuk, Tabuk 71451
[57] Tata Institute of Fundamental Research, Mumbai 400005
[58] Excellence Cluster Universe, Technische Universität München, 85748 Garching
[59] Toho University, Funabashi 274-8510
[60] Tohoku Gakuin University, Tagajo 985-8537
[61] Tohoku University, Sendai 980-8578
[62] Department of Physics, University of Tokyo, Tokyo 113-0033
[63] Tokyo Institute of Technology, Tokyo 152-8550
[64] Tokyo Metropolitan University, Tokyo 192-0397
[65] Tokyo University of Agriculture and Technology, Tokyo 184-8588
[66] University of Torino, 10124 Torino
[67] CNP, Virginia Polytechnic Institute and State University, Blacksburg, Virginia 24061
[68] Wayne State University, Detroit, Michigan 48202
[69] Yamagata University, Yamagata 990-8560
[70] Yonsei University, Seoul 120-749

(Dated: March 3, 2014)

We report the first measurement of the lepton forward-backward asymmetry $\mathcal{A}_{\rm FB}$ for the inclusive electroweak penguin process $B \to X_s \ell^+ \ell^-$ as a function of $q^2 = M^2_{\ell^+\ell^-} c^2$, where $\ell$ is an electron or a muon and $X_s$ is a hadronic recoil system with an $s$ quark. The results are based on a data sample containing $772 \times 10^6$ $B\bar{B}$ pairs recorded at the $\Upsilon(4S)$ resonance with the Belle detector at the KEKB $e^+e^-$ collider. For $q^2 > 10.2$ GeV$^2/c^2$, $\mathcal{A}_{\rm FB} < 0$ is excluded at the $2.3\sigma$ level, where $\sigma$ is the standard deviation. For $q^2 < 4.3$ GeV$^2/c^2$, the result is within $1.8\sigma$ of the theoretical expectation.

PACS numbers: 11.30.Er, 11.30.Hv, 12.15.Ji, 13.20.He

In the Standard model (SM), quark-level flavor-changing neutral current $b \to s\ell^+\ell^-$ decays [1] are allowed at higher order via the electroweak loop (penguin) and $W^+W^-$ box diagrams. The corresponding decay amplitude can be expressed via the Operator Product Expansion [2] in terms of the effective Wilson coefficients for the electromagnetic penguin, $C_7^{\rm eff}$, and the vector and axial-vector electroweak contributions, $C_9^{\rm eff}$ and $C_{10}^{\rm eff}$, respectively [3]. If physics beyond the SM contributes to $b \to s\ell^+\ell^-$ decays, then the effective Wilson coefficients are expected to differ from the SM expectations. Therefore the decay rate and angular distributions of $b \to s\ell^+\ell^-$ decays constitute good probes to search for new physics [4].

Inclusive measurements of the $b \to s\ell^+\ell^-$ process are preferable to exclusive measurements because of lower theoretical uncertainties, although they are experimentally more challenging. The branching fraction for inclusive $B \to X_s\ell^+\ell^-$, where $B$ is either $\bar{B}^0$ or $B^-$, $\ell$ is either an electron or a muon, and $X_s$ is a hadronic recoil system with an $s$ quark, has been measured by Belle [5] and *BABAR* [6]. Both results are consistent with the

SM prediction. The lepton forward-backward asymmetry, defined as

$$\mathcal{A}_{\rm FB}(q^2_{\rm min}, q^2_{\rm max}) = \frac{\int_{q^2_{\rm min}}^{q^2_{\rm max}} dq^2 \int_{-1}^{1} d\cos\theta\, {\rm sgn}(\cos\theta) \frac{d^2\Gamma}{dq^2 d\cos\theta}}{\int_{q^2_{\rm min}}^{q^2_{\rm max}} dq^2 \int_{-1}^{1} d\cos\theta \frac{d^2\Gamma}{dq^2 d\cos\theta}}$$

is considered to have different and greater sensitivity to physics beyond the SM than the branching fraction [7]. Here, $q^2 = M^2_{\ell^+\ell^-}c^2$ and $\theta$ is the angle between the $\ell^+(\ell^-)$ and the $B$ meson momentum in the $\ell^+\ell^-$ center-of-mass frame in $\bar{B}^0$ or $B^-$ ($B^0$ or $B^+$) decays. Although $\mathcal{A}_{\rm FB}$ in exclusive $B \to K^{(*)}\ell^+\ell^-$ has been measured by Belle [8], *BABAR* [9], CDF [10], LHCb [11] and CMS [12], $\mathcal{A}_{\rm FB}$ in inclusive $B \to X_s\ell^+\ell^-$ is yet to be measured.

In this Letter, we report the first measurement of the lepton forward-backward asymmetry for inclusive $B \to X_s\ell^+\ell^-$, assuming $\mathcal{A}_{\rm FB}$ does not depend on the lepton flavor. The results are based on the full $\Upsilon(4S)$ data sample containing $772 \times 10^6$ $B\bar{B}$ pairs recorded with the Belle detector [13] at the KEKB $e^+e^-$ collider [14].

We study the acceptance for $B \to X_s\ell^+\ell^-$ via Monte Carlo (MC) simulation. For this simulation, we use a sum of exclusive $B \to K^{(*)}\ell^+\ell^-$ events and non-resonant $B \to X_s\ell^+\ell^-$ events with the $X_s$ invariant mass $M_{X_s} > 1.1$ GeV/$c^2$. The former are generated according to Refs. [4, 15], while the latter are generated using a model based on Refs. [4, 16] and the Fermi motion model of Ref. [17]. The two MC samples are mixed assuming the measured branching fractions [18].

Charged tracks are reconstructed with the silicon vertex detector (SVD) and central drift chamber (CDC), and the tracks other than $K^0_S \to \pi^+\pi^-$ daughters are required to originate from the interaction region. Electrons are identified by a combination of the specific ionization ($dE/dx$) in the CDC, the ratio of the cluster energy in the electromagnetic calorimeter (ECL) to the track momentum measured with the SVD and CDC, the response of the aerogel threshold Cherenkov counters (ACC), the shower shape in the ECL, and position matching between the shower and the track. Muons are identified by the track penetration depth and hit scatter in the muon detector (KLM). Electrons and muons are required to have momenta greater than 0.4 GeV/$c$ and 0.8 GeV/$c$, respectively. To recover bremsstrahlung photons from leptons, we add the four-momentum of each photon detected within 0.05 rad of the original track direction. Charged kaons are identified by combining information from the $dE/dx$ in the CDC, the flight time measured with the time-of-flight scintillation counters (TOF), and the response of the ACC [19]. We select electron, muon, and kaon candidate tracks in turn, while the remaining tracks are assumed to be charged pions.

$K^0_S$ candidates are formed by combining two oppositely charged tracks, assuming both are pions with requirements on their invariant mass, flight length, and consistency between the $K^0_S$ momentum direction and vertex position. Neutral pion candidates are formed from pairs of photons that have an invariant mass within 10 MeV/$c^2$ of the nominal $\pi^0$ mass, where photons are measured as an energy cluster in the ECL with no associated charged tracks. Neutral pions and their photon daughters are required to have an energy greater than 400 MeV and 50 MeV, respectively. A mass-constrained fit is then performed to obtain the $\pi^0$ momentum.

TABLE I. The 18 hadronic final states used to reconstruct $X_s$. The 8 final states enclosed in parentheses are not used for the measurement of $\mathcal{A}_{\rm FB}$.

| $\bar{B}^0$ decays | | $B^-$ decays | |
|---|---|---|---|
| | $(K^0_S)$ | $K^-$ | |
| $K^-\pi^+$ | $(K^0_S\pi^0)$ | $K^-\pi^0$ | $K^0_S\pi^-$ |
| $K^-\pi^+\pi^0$ | $(K^0_S\pi^-\pi^+)$ | $K^-\pi^+\pi^-$ | $K^0_S\pi^-\pi^0$ |
| $K^-\pi^+\pi^-\pi^+$ | $(K^0_S\pi^-\pi^+\pi^0)$ | $K^-\pi^+\pi^-\pi^0$ | $K^0_S\pi^-\pi^+\pi^-$ |
| $(K^-\pi^+\pi^-\pi^+\pi^0)$ | $(K^0_S\pi^-\pi^+\pi^-\pi^+)$ | $(K^-\pi^+\pi^-\pi^+\pi^-)$ | $(K^0_S\pi^-\pi^+\pi^-\pi^0)$ |

We reconstruct $X_s$ from 18 hadronic final states (see Table I), that consist of one $K^\pm$ or $K^0_S$ and up to four pions, of which at most one can be neutral. We require $M_{X_s} < 2$ GeV/$c^2$ to reject a large part of the combinatorial background.

We combine the $X_s$ with two oppositely charged leptons to form a $B$ meson candidate. To identify the signal, we use two kinematic variables defined in the $\Upsilon(4S)$ rest frame: the beam-energy constrained mass $M_{\rm bc} = \sqrt{E^{*2}_{\rm beam} - |\vec{p}_B|^2}$, and the energy difference $\Delta E = E_B - E^*_{\rm beam}$, where $E^*_{\rm beam}$ is the beam energy and $(\vec{p}_B, E_B)$ is the reconstructed momentum and energy of the $B$ candidate. We require $M_{\rm bc} > 5.22$ GeV/$c^2$ and $-100$ MeV $< \Delta E < 50$ MeV ($-50$ MeV $< \Delta E < 50$ MeV) for the electron (muon) channel.

To reject large contamination from charmonium backgrounds $B \to J/\psi(\psi(2S))X_s$ following $J/\psi(\psi(2S)) \to \ell^+\ell^-$, we reject events having dilepton invariant mass in the following veto regions: $-400$ to 150 MeV/$c^2$ ($-250$ to 100 MeV/$c^2$) around the $J/\psi$ mass and $-250$ to 100 MeV/$c^2$ ($-150$ to 100 MeV/$c^2$) around the $\psi(2S)$ mass for the electron (muon) channel. In the electron channel, there is non-negligible peaking background from events in which the bremsstrahlung photon recovery fails and instead the radiated photon together with another random photon forms a misreconstructed $\pi^0$ as $X_s$'s daughter. To veto such events, the $\pi^0$'s photon daughter with the highest energy is added in the calculation of the dilepton invariant mass, and events with invariant mass from 150 MeV/$c^2$ below to 50 MeV/$c^2$ above the nominal $J/\psi$ mass are rejected for the modes involving $\pi^0$. We also require the dilepton mass to be greater than 0.2 GeV/$c^2$ to remove the photon conversion and $\pi^0$ Dalitz decays.

The main background comes from random combinations of two semileptonic $B$ or $D$ decays, which have both large missing energy due to neutrinos, and displaced origin of leptons from $B$ or $D$ mesons. The displacement be-

tween the two leptons is measured by the distance $\Delta z_{\ell^+\ell^-}$ between the points of closest approach to the beam axis along the beam direction. We also use the confidence level of the $B$ vertex ($\mathcal{C}_{\rm vtx}$), constructed from all charged daughter particles except for $K^0_S$ daughters. We set requirements on $\Delta z_{\ell^+\ell^-}$ and $\mathcal{C}_{\rm vtx}$ to preserve about 79% of the signal while rejecting 66% of the background. Other background originates from $e^+e^- \to q\bar{q}$ ($q = u, d, s, c$) continuum events, which can be efficiently suppressed using event shape variables.

To suppress the continuum background and further reduce the semileptonic background, we employ a neural network based on the software package "NeuroBayes" [20]. The inputs to the network are (i) a likelihood ratio based on $\Delta E$, (ii) the cosine of the angle between the $B$ candidate and the beam axis in the $\Upsilon(4S)$ rest frame, (iii) $\Delta z_{\ell^+\ell^-}$, (iv) $\mathcal{C}_{\rm vtx}$, (v) the total visible energy, (vi) the missing mass [21], and (vii) 17 event shape variables based on modified Fox-Wolfram moments [22]. For the different types of backgrounds (semileptonic and continuum), the neural network is trained separately and requirements on two output values are chosen to maximize the statistical significance. This optimization is performed separately for electron and muon channels and for the regions $M_{X_s} < 1.1$ GeV/$c^2$ and $M_{X_s} > 1.1$ GeV/$c^2$, and the obtained selection preserves 51% (63%) of the signal while rejecting 98% (96%) of the background for electron (muon) channels. According to the MC simulation, 83% of the remaining background consists of semileptonic events.

There are three peaking background sources: charmonium background from $B \to J/\psi(\psi(2S))X_s$ decays with $J/\psi(\psi(2S)) \to \ell^+\ell^-$, $B \to D^{(*)}n\pi$ ($n > 0$) decays with two misidentified charged pions as leptons, and $B \to J/\psi(\psi(2S))X_s$ decays with swapped misidentification of a lepton and a pion. The first of these peaking backgrounds is studied with MC events, while the others are determined from data. We treat contributions from charmonium resonances higher than $\psi(2S)$ as signal.

The probability of multiple $B$ candidates in an event is 8% with the average number of $B$ candidates per event being 1.1. When multiple $B$ candidates are found in an event, we select the most signal-like $B$ candidate based on the neural network output. For the measurement of $\mathcal{A}_{\rm FB}$, information on the flavor of the $B$ candidate is necessary. For $\bar{B}^0$ mesons, only the self-tagging modes with a $K^-$ are kept, after selecting one $B$ candidate per event. We also remove candidates with $X_s$ reconstructed from one kaon plus four pions because expected signal yields are less than one event. Therefore, we use 10 final states as listed in Table I for the $X_s$ to measure $\mathcal{A}_{\rm FB}$.

To examine the $q^2$ dependence of $\mathcal{A}_{\rm FB}$, we divide the data into 4 bins of measured $q^2$: [0.2, 4.3], [4.3, 7.3(8.1)], [10.5(10.2), 11.8(12.5)], [14.3, 25.0] GeV$^2/c^2$ for the electron (muon) channel, where the gap regions correspond to the veto regions for charmonium background events. In order to extract $\mathcal{A}_{\rm FB}$, an extended unbinned maximum likelihood fit to four $M_{\rm bc}$ distributions (positive/negative $\cos\theta$ for electron/muon channel) is simultaneously performed for each $q^2$ bin. The signal reconstruction efficiency highly depends on $q^2$ and $\cos\theta$, as events with low $q^2$ and high $\cos\theta$ have lepton momenta below those required in the event selection. This leads to a deviation of $\mathcal{A}_{\rm FB}^{\rm raw} = \frac{N(\cos\theta>0)-N(\cos\theta<0)}{N(\cos\theta>0)+N(\cos\theta<0)}$ from $\mathcal{A}_{\rm FB}$, where $N$ is the observed number of signal events. The relation between $\mathcal{A}_{\rm FB}$ and $\mathcal{A}_{\rm FB}^{\rm raw}$ is expressed as,

$$\begin{aligned}\mathcal{A}_{\rm FB} &= \alpha^{\mu\mu} \cdot \mathcal{A}_{\rm FB}^{{\rm raw},\mu\mu} \\ &= \alpha^{ee} \cdot \beta \cdot \mathcal{A}_{\rm FB}^{{\rm raw},ee}, \end{aligned} \quad (1)$$

assuming $\mathcal{A}_{\rm FB}$ does not depend on the lepton flavor. Here, $\alpha$ is a scaling factor that relates $\mathcal{A}_{\rm FB}^{\rm raw}$ with $\mathcal{A}_{\rm FB}$ and $\beta$ is the correction factor from electron channels to muon channels. In the 2nd and 3rd $q^2$ bins, $\mathcal{A}_{\rm FB}$ is different between electron and muon channels, due to the different charmonium veto regions. We use $\mathcal{A}_{\rm FB}$ of Eq. (1) defined for the $q^2$ regions of the muon channel as the fit parameter. To derive $\alpha$, we generate several sets of signal MC samples with various Wilson coefficients ($C_7$, $C_9$, $C_{10}$), calculate $\mathcal{A}_{\rm FB}$ and $\mathcal{A}_{\rm FB}^{\rm raw}$ for each set, and fit the relation between them by a straight line. To derive $\beta$, we fit the relation between forward-backward asymmetry calculated using the $q^2$ region in the electron and muon channels in the same way. The values of $\alpha$ and $\beta$ are summarized in Table II.

The likelihood function consists of four components: signal, self cross-feed, combinatorial background, and peaking background. The signal is modeled with a Gaussian function with parameters obtained from the $B \to J/\psi X_s$ data. The self cross-feed is described by a MC histogram, where the yield ratio to the signal is fixed according to the MC expectation. The combinatorial background is modeled by an ARGUS function [23], where the endpoint is fixed to the nominal beam energy in the $\Upsilon(4S)$ rest frame, $E^*_{\rm beam} = 5.289$ GeV. The size of the sum of the peaking backgrounds is fixed in the fit to $1.0 \pm 0.2$ and $11.4 \pm 0.3$ events for the electron and muon channels, respectively.

Figure 1 shows the $M_{\rm bc}$ distributions for $B \to X_s e^+e^-$ and $B \to X_s \mu^+\mu^-$ candidates with positive and negative $\cos\theta$. The total signal yields for $B \to X_s e^+e^-$ and $B \to X_s \mu^+\mu^-$ are 140 $\pm$ 19(stat) and 161 $\pm$ 20(stat), respectively. The fit results obtained in each of the four $q^2$ bins are summarized in Table II. Figure 2 shows the $\mathcal{A}_{\rm FB}$ distribution as a function of $q^2$. To see contributions from events other than $B \to K^{(*)}\ell^+\ell^-$ candidates, we select samples with $M_{X_s} > 1.1$ GeV/$c^2$, and extract $\mathcal{A}_{\rm FB}$ by the same fitting method. As a result, we obtain $\mathcal{A}_{\rm FB} = 0.25 \pm 0.45$ (1st bin), $0.97 \pm 0.60$ (2nd bin), $0.92 \pm 0.32$ (3rd bin), and $0.65 \pm 0.54$ (4th bin), where only the statistical uncertainties are listed.

To estimate systematic uncertainties, we repeat the $\mathcal{A}_{\rm FB}$ fit with varied input parameters and the resulting

TABLE II. Fit results for the four $q^2$ bins. For $\mathcal{A}_{\rm FB}$, the first uncertainty is statistical and the second uncertainty is systematic. $\mathcal{A}_{\rm FB}$ values predicted by the SM [4, 7] are also shown with systematic uncertainties. For the signal yields, only statistical uncertainties are shown. The uncertainties of $\alpha$ and $\beta$ are due to the statistical uncertainties of the MC.

| | 1st bin | 2nd bin | 3rd bin | 4th bin |
|---|---|---|---|---|
| $q^2$ range [GeV$^2/c^2$] $(B \to X_s e^+ e^-)$ | [0.2,4.3] | [4.3,7.3] | [10.5,11.8] | [14.3, 25.0] |
| $q^2$ range [GeV$^2/c^2$] $(B \to X_s \mu^+ \mu^-)$ | | [4.3,8.1] | [10.2,12.5] | |
| $\mathcal{A}_{\rm FB}$ | $0.34 \pm 0.24 \pm 0.02$ | $0.04 \pm 0.31 \pm 0.05$ | $0.28 \pm 0.21 \pm 0.01$ | $0.28 \pm 0.15 \pm 0.01$ |
| $\mathcal{A}_{\rm FB}$ (theory) | $-0.11 \pm 0.03$ | $0.13 \pm 0.03$ | $0.32 \pm 0.04$ | $0.40 \pm 0.04$ |
| $N_{\rm sig}^{ee}$ | $45.6 \pm 10.9$ | $30.0 \pm 9.2$ | $25.0 \pm 7.0$ | $39.2 \pm 9.6$ |
| $N_{\rm sig}^{\mu\mu}$ | $43.4 \pm 9.2$ | $23.9 \pm 10.4$ | $30.7 \pm 9.9$ | $62.8 \pm 10.4$ |
| $\alpha^{ee}$ | $1.289 \pm 0.004$ | $1.139 \pm 0.003$ | $1.063 \pm 0.003$ | $1.121 \pm 0.003$ |
| $\alpha^{\mu\mu}$ | $2.082 \pm 0.010$ | $1.375 \pm 0.003$ | $1.033 \pm 0.003$ | $1.082 \pm 0.003$ |
| $\beta$ | 1.000 | $1.019 \pm 0.003$ | $1.003 \pm 0.000$ | 1.000 |

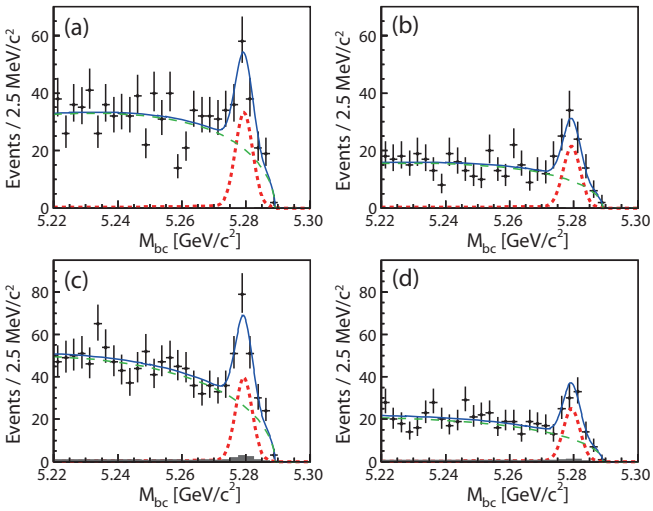


FIG. 1. $M_{\rm bc}$ distributions for (a) $B \to X_s e^+ e^-$ candidates with $\cos\theta > 0$, (b) $B \to X_s e^+ e^-$ candidates with $\cos\theta < 0$, (c) $B \to X_s \mu^+ \mu^-$ candidates with $\cos\theta > 0$, and (d) $B \to X_s \mu^+ \mu^-$ candidates with $\cos\theta < 0$. The thicker dashed curve (red) shows the sum of the signal and the self cross-feed components. The thinner dashed curve (green) shows the combinatorial background component. The filled histogram (gray) shows the peaking background component. The sums of all components are shown by the solid curve (blue).

change in $\mathcal{A}_{\rm FB}$ is taken as the systematic uncertainty for the varied parameter. Systematic uncertainties for $\mathcal{A}_{\rm FB}$ are summarized in Table III. In the 1st and 3rd $q^2$ bins, the dominant systematic uncertainty arises from the translation of $\mathcal{A}_{\rm FB}^{\rm raw}$ to $\mathcal{A}_{\rm FB}$ with $\alpha$ and $\beta$. Even if a MC sample with a different set of Wilson coefficients produces the same values of $\mathcal{A}_{\rm FB}$, the $\mathcal{A}_{\rm FB}^{\rm raw}$ values and hence the $\alpha$ coefficient may differ. It gives rise to an uncertainty of the offset in the linear fit. To estimate this uncertainty, the relation between $\mathcal{A}_{\rm FB}^{\rm raw}$ and $\mathcal{A}_{\rm FB}$ are projected onto the axis perpendicular to the fitted linear line and fitted by a Gaussian function. To estimate systematic uncertainties from the peaking background, the yield of each such background is varied by its uncertainty. For the charmonium peaking background, the yield is varied by $\pm 100\%$, conservatively, because it is determined from MC events. A possible peaking background from $B \to Kn\pi\ell\nu (n > 0)$, where one pion is misidentified as a lepton and the missing neutrino is compensated by a pion of the other $B$ decay, is examined. The number of events in the whole $q^2$ region is estimated from MC to be $0.2 \pm 0.6$ $(1.1 \pm 0.7)$ for electron (muon) channel, and the resulting systematic error is $\mathcal{O}(0.001)$. To estimate the systematic uncertainties from signal modeling, the related parameters are varied. The fraction of $B \to K^{(*)}\ell^+\ell^-$ and non-resonant $B \to X_s \ell^+ \ell^-$ are varied within experimental uncertainties. The Fermi motion parameter is varied

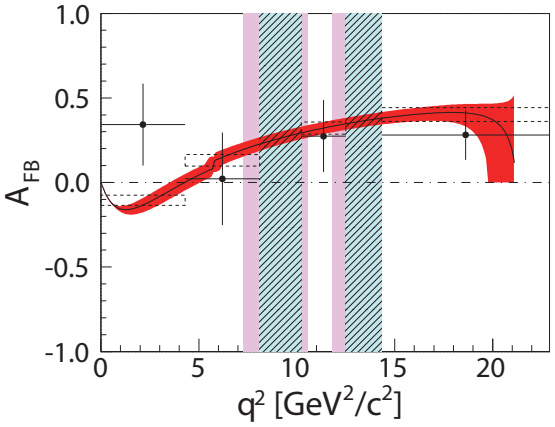


FIG. 2. Measured $\mathcal{A}_{\rm FB}$ as a function of $q^2$. The curve (black) with the band (red) and dashed boxes (black) represent the SM prediction while filled circles with error bars show the fit results. The $J/\psi$ and $\psi(2S)$ veto regions are shown as teal hatched regions. For the electron channel, the pink shaded regions are added to the veto regions due to the large bremsstrahlung effect. The uncertainty on the SM prediction is estimated by varying the $b$-quark mass ($4.80 \pm 0.15$ GeV/$c^2$), the $s$-quark mass ($0.20 \pm 0.10$ GeV/$c^2$), and the renormalization scale ($\mu = 2.5$ and 5 GeV) [4, 7]. The lower edge of the uncertainty is set to zero in the uncomputable region.

TABLE III. Summary of systematic uncertainties in the four $q^2$ bins.

| Sources of uncertainties | 1st | 2nd | 3rd | 4th |
|---|---|---|---|---|
| Translation from $\mathcal{A}_{\rm FB}^{\rm raw}$ to $\mathcal{A}_{\rm FB}$ | 0.019 | 0.013 | 0.007 | 0.003 |
| Peaking background | 0.004 | 0.050 | 0.007 | 0.002 |
| Signal modeling | 0.004 | 0.002 | 0.006 | 0.006 |
| Signal shape and self cross-feed | 0.002 | 0.002 | 0.002 | 0.002 |
| Total | 0.020 | 0.052 | 0.012 | 0.007 |

in accordance with measurements of hadronic moments in semileptonic $B$ decays [24] and the photon spectrum in inclusive $B \to X_s\gamma$ decays [25]. The $b$-quark pole mass is varied by $\pm 0.15$ GeV/$c^2$ around 4.80 GeV/$c^2$. The threshold point of non-resonant $B \to X_s\ell^+\ell^-$ events is varied by $\pm 100$ MeV/$c^2$ around $M_{X_s} = 1.1$ GeV/$c^2$. We check the hadronization process in the non-resonant $B \to X_s\ell^+\ell^-$ events by comparing the $B \to J/\psi X_s$ events in data and MC simulations. To estimate the systematic uncertainties related to $X_s$ spin components, we generate the non-resonant $B \to X_s\ell^+\ell^-$ MC samples with spin 0 and 1 using the form factor for $B \to K^{(*)}\ell^+\ell^-$ and vary the fractions of each spin component as a linear function of $M_{X_s}$, by up to $\pm 10\%$ in the range of [1.1, 2.0] GeV/$c^2$. The signal shape parameters are fixed using the $J/\psi X_s$ data. The mean and width of the signal Gaussian function are varied within their uncertainties. The histogram shape of the self cross-feed background is estimated from signal MC events. The entries in the bins are varied according to a Gaussian distribution whose standard deviation is the statistical uncertainty of the MC sample. The total systematic uncertainty is estimated by summing the above uncertainties in quadrature.

The $\mathcal{A}_{\rm FB}$ results are found to be consistent with the SM prediction in the 2nd to 4th $q^2$ bins, while it deviates from the SM in the 1st $q^2$ bin by $1.8\sigma$; here, the systematic uncertainty is taken into account. The results in the 3rd and 4th bin also excludes $\mathcal{A}_{\rm FB} < 0$ at the $2.3\sigma$ level.

In conclusion, we report the first measurement of the lepton forward-backward asymmetry for the inclusive electroweak penguin process $B \to X_s\ell^+\ell^-$ using a data sample containing $772 \times 10^6$ $B\bar{B}$ pairs collected with the Belle detector. For $q^2 > 10.2$ GeV$^2/c^2$, $\mathcal{A}_{\rm FB} < 0$ is excluded at the $2.3\sigma$ level. For $q^2 < 4.3$ GeV$^2/c^2$, the result is within $1.8\sigma$ of the SM expectation. The results can be used to constrain various extensions of the SM.

We thank T. Morozumi and T. Goto for their invaluable suggestions. We thank the KEKB group for excellent operation of the accelerator; the KEK cryogenics group for efficient solenoid operations; and the KEK computer group, the NII, and PNNL/EMSL for valuable computing and SINET4 network support. We acknowledge support from MEXT, JSPS and Nagoya's TLPRC (Japan); ARC and DIISR (Australia); FWF (Austria); NSFC (China); MSMT (Czechia); CZF, DFG, and VS (Germany); DST (India); INFN (Italy); MEST, NRF, GSDC of KISTI, and WCU (Korea); MNiSW and NCN (Poland); MES and RFAAE (Russia); ARRS (Slovenia); IKERBASQUE and UPV/EHU (Spain); SNSF (Switzerland); NSC and MOE (Taiwan); and DOE and NSF (USA).

[1] Charge-conjugate decays are implied throughout this paper, unless otherwise stated.
[2] K. G. Wilson, Phys. Rev. **179**, 1499 (1969).
[3] G. Buchalla, A.J. Buras, and M.E. Lautenbacher, Rev. Mod. Phys. **68**, 1125 (1996).
[4] A. Ali, E. Lunghi, C. Greub, and G. Hiller, Phys. Rev. **D66**, 034002 (2002).
[5] M. Iwasaki *et al.* (Belle Collaboration), Phys. Rev. **D72**, 092005 (2005).
[6] B. Aubert *et al.* (*BABAR* Collaboration), Phys. Rev. Lett. **93**, 081802 (2004).
[7] S. Fukae, C.S. Kim, T. Morozumi, and T. Yoshikawa, Phys. Rev. **D59**, 074013 (1999).
[8] J.-T. Wei *et al.* (Belle Collaboration), Phys. Rev. Lett. **103**, 171801 (2009).
[9] B. Aubert, *et al.* (*BABAR* Collaboration), Phys. Rev. **D79**, 031102(R) (2009).
[10] T. Aaltonen *et al.* (CDF Collaboration), Phys. Rev. Lett. **108**, 081807 (2012).
[11] R. Aaij *et al.* (LHCb Collaboration), Phys. Rev. Lett. **108**, 181806 (2012).
[12] S. Chatrchyan *et al.* CMS Collaboration, Phys. Lett. **B727**, 77 (2013).
[13] A. Abashian *et al.* (Belle Collaboration), Nucl. Instrum. Methods Phys. Res., Sect. A **479**, 117 (2002); also see the detector section in J. Brodzicka *et al.*, Prog. Theor. Exp. Phys. (2012) 04D001.
[14] S. Kurokawa and E. Kikutani, Nucl. Instrum. Methods Phys. Res., Sect. A **499**, 1 (2003), and other papers included in this volume; T. Abe *et al.*, Prog. Theor. Exp. Phys. (2013) 03A001 and following articles up to 03A011.
[15] A. Ali, P. Ball, L.T. Handoko, and G. Hiller, Phys. Rev. **D61**, 074024 (2000).
[16] F. Kruger and L.M. Sehgal, Phys. Lett. **B380**, 199 (1996).
[17] A. Ali and E. Pietarinen, Nucl. Phys. **B154**, 519 (1979).
[18] Y. Amhis *et al.*, arXiv:1207.1158 and online update at http://www.slac.stanford.edu/xorg/hfag/
[19] E. Nakano, Nucl. Instrum. Methods Phys. Res., Sect. A **494**, 402 (2002).
[20] M. Fiendt and U. Kerzel, Nucl. Instrum. Methods Phys. Res., Sect. A **559**, 190 (2006).
[21] We define the total visible energy $E_{\rm vis} = \sum_i E_i^*$, and the missing mass $M_{\rm miss} = \sqrt{(2E_{\rm beam}^* - \sum_i E_i^*)^2 - \sum_i |\vec{p}_i^*|^2}$, where $(\vec{p}_i^*, E_i^*)$ are the reconstructed four-momenta in the $\Upsilon(4S)$ rest frame of all tracks assumed to be pions and all photons in the event.
[22] The Fox-Wolfram moments were introduced in G.C. Fox and S. Wolfram, Phys. Rev. Lett. **41**, 1581 (1978); The modified moments used in this Letter are described in S.H. Lee *et al.* (Belle Collaboration), Phys. Rev. Lett. **91**, 261801 (2003).
[23] H. Albrecht *et al.* (ARGUS Collaboration), Phys. Lett. B **241**, 278 (1990).

[24] C. Schwanda *et al.* (Belle Collaboration) Phys. Rev. **D75**, 032005 (2007).

[25] A. Limosani *et al.* (Belle Collaboration) Phys. Rev. Lett. **103**, 241801 (2009).